Supplementary material

Gamma-secretase inhibitors reverse glucocorticoid resistance in T-ALL.

Pedro J. Real, Valeria Tosello, Teresa Palomero, Mireia Castillo, Eva Hernando-Monge, Elisa de Stanchina, Maria Luisa Sulis, Kelly Barnes, Catherine Sawai, Irene Homminga, Jules Meijerink, Iannis Aifantis, Giuseppe Basso, Carlos Cordon-Cardo, Walden Ai and Adolfo Ferrando.

Supplementary results and discussion

Treatments that target the aberrant signaling pathways controlling the growth and survival of malignant T-lymphoblasts are attracting wide attention as promising tools in the therapeutic armamentarium for human leukemias. The rationale for inhibiting oncogenic pathways in anticancer therapy is based on the concept of oncogene addiction, which posits that cancer cells become dependent on continuous oncogenic signals for proliferation and survival, as well as experimental evidence linking oncogenic pathways with chemotherapy resistance [1,2]. Thus, the combination of molecularly targeted drugs with conventional antileukemic agents could provide an improved therapeutic window with increased efficacy and reduced toxicity.

The data we report substantiates this prediction, showing that inhibition of NOTCH1 signaling can effectively abrogate glucocorticoid resistance in T-ALL primary patient samples and cell lines.

Despite numerous studies addressing the mechanisms that mediate the response of leukemia cells to glucocorticoid therapy, the molecular basis of glucocorticoid resistance remains incompletely understood [3-20]. In this context, our results identify a transcriptional regulatory circuit that controls glucocorticoid receptor expression and glucocorticoid receptor auto-upregulation downstream of oncogenic NOTCH1 as a potential therapeutic target to reverse glucocorticoid resistance in T-ALL.

This mechanism, which was characterized in detail in the immortalized CUTLL1 cells, was also verified in leukemic lymphoblasts from the original lymphoma sample used to generate this cell line (T-ALL sample 2, **Fig. 1c, Supplementary Fig.3b**), indicating that the mechanistic interplay between NOTCH1 signaling, glucocorticoid receptor auto upregulation and glucocorticoid resistance were original features of these glucocorticoid-resistant tumor cells. Furthermore, the combination of glucocorticoids with GSIs was strongly synergistic, shifting the effects of GSI treatment from mildly cytostatic to strongly cytotoxic.

To test the specificity of the interaction between GSIs and glucocorticoids, we analyzed the effects of GSI treatment in the response of CUTLL1 cells to a panel of antineoplastic drugs with different mechanisms of action. These experiments showed that in contrast to the synergistic effects of CompE and dexamethasone, γ-secretase inhibition did not influence the apoptotic responses triggered by etoposide, vincristine, L-asparaginase or methotrexate in T-ALL (**Supplementary Fig. 5** online). Similar results were obtained in KOPTK1 and TALL1 cells (data not shown). From these results, we concluded that GSI treatment sensitizes T-ALL lymphoblasts specifically to glucocorticoid-induced cell death by a mechanism that does not affect the sensitivity of these cells to apoptosis induced by double-strand DNA breaks (etoposide), spindle dysfunction (vincristine), inhibition of protein biosynthesis (L-asparaginase), or a block of nucleotide metabolism (methotrexate).

Numerous studies on the mechanisms of action of glucocorticoids have demonstrated an important role of the mitochondrial apoptotic pathway in the activation of glucocorticoid-induced cell death [6]. The synergistic effects of GSI-treatment and glucocorticoids were mediated by improved glucocorticoid receptor auto-up-regulation leading to effective upregulation of *BIM*, a proapoptotic BH3-only factor previously implicated in glucocorticoid-induced cell death (**Fig. 3h**) [21-23]. Extended expression analysis of all major apoptosis regulators of the BCL2 and BH3 only subfamilies failed to identify any other significant changes in gene expression potentially associated with an increased cell death response (data not shown).

Additional pharmacologic interactions affecting glucocorticoid resistance in ALL have been described before. Most notably, inhibition of mTOR signaling with rapamycin can reverse glucocorticoid resistance in leukemic lymphoblasts inducing posttranscriptional downregulation of MCL1 [20], however, we failed to detect changes in the protein levels of this antiapoptotic factor in cells treated with CompE plus dexamethasone (data not shown). Similarly, we did not detect changes in the differentiation arrest of T-ALL cells that could be linked to differential glucocorticoid sensitivity or transcriptional changes in the *SRG3* gene (data not shown), two mechanisms proposed to reduce the sensitivity to glucocorticoid-induced apoptosis downstream of NOTCH1 activation in mouse primary thymocytes [24-27].

In vivo studies using a mouse xenograft model of T-ALL demonstrated an increased antitumor effect in animals treated with DBZ plus dexamethasone. Importantly 6/8 animals engrafted with glucocorticoid resistant T-ALL cells and treated with DBZ plus dexamethasone remained leukemia free by bioimaging analysis at 8 weeks post-treatment. Furthermore, minimal residual disease levels in this group were below the level of detection as established by flow cytometric analysis of spleen cells after anti-human CD45 staining, confirming complete clearance of human leukemic cells in animals treated with DBZ plus dexamethasone (data not shown).

A surprising observation during these *in vivo* studies was an accelerated mortality in the DBZ only treatment group, presumably associated with the development of GSI induced toxicity, that was effectively reversed in animals treated with DBZ plus dexamethasone. The enteroprotective effects of dexamethasone against DBZ induced gut toxicity were validated histologically and clinically in extended analysis of the effects of DBZ treatment in non leukemia bearing mice.

Analysis C57/Bl6 mice treated with vehicle only (DMSO), dexamethasone (15 mg/kg), DBZ (10 μM/kg) or dexamethasone (15 mg/kg) plus DBZ (10 μM/kg) via intraperitoneal injection daily for 5 and 10 days showed a marked reduction in the gastrointestinal toxicity with reversal

of the proliferative arrest and intestinal secretory metaplasia typically induced by GSI treatment when mice were cotreated with a glucocorticoid (dexamethasone) (**Fig.4** and **Supplementary Figs. 10** and **11** online). Notably, detailed histological analysis of dexamethasone treated animals showed that glucocorticoid treatment induces increased Paneth cell differentiation and increased proliferation in the intestinal crypts, which show an elongated morphology, contain 20-30% more cells ($P < 0.001$) and have increased numbers of Ki67 positive cells per crypt ($P < 0.001$). These histological changes are most evident after 10 days of treatment as shown in **Figure 6d** and **Supplementary Figure 11**. These results highlight a previously unrealized role for glucocorticoids in the control of cell proliferation and cell fate decisions in the gut.

These studies also revealed that both dexamethasone and DBZ treatment induced thymic atrophy with depletion of cortical thymocytes, which was more severe in animals treated with DBZ plus dexamethasone (**Fig. 4e** and **Supplementary Fig. 13** online). In the spleen, DBZ induced disappearance of the marginal zone in the white pulp (**Fig. 4e** and **Supplementary Fig. 14** online), a defect typically associated with loss of NOTCH signaling [28,29]. Mice treated with dexamethasone showed moderate atrophy of the white pulp with preservation of the marginal zone and disorganization of the red pulp (**Fig. 4e** and **Supplementary Fig. 14** online). By contrast, dexamethasone plus DBZ produced severe alterations of the splenic architecture, characterized by marked lymphoid atrophy and disappearance of the marginal zone in the white pulp and prominent disorganization of the red pulp (**Fig. 4e** and **Supplementary Fig. 14** online). Importantly, although the combination of dexamethasone with DBZ also resulted in increased lymphoid depletion in the thymus and the spleen, these changes were not associated with any clinical symptoms. In addition, these effects of dexamethasone plus DBZ treatment in lymphoid tissues were reversible as demonstrated by restored organ size and cellularity with complete repletion of double positive T-cells and marginal zone B cells in the thymus and the spleen, respectively (**Supplementary Figs. 13,14** online).

Clinical follow-up of C57/Bl6 mice treated with vehicle only (DMSO), dexamethasone (15 mg kg^{-1}), DBZ (10 μM/kg) or dexamethasone (15 mg/kg) plus DBZ (10 μM/kg) via intraperitoneal injection daily treated for extended periods of time showed that 100% of DBZ treated animals developed mucous diarrhea after two weeks of treatment, which is consistent with the development of intestinal secretory metaplasia characteristic of GSI-induce gut toxicity. Notably, mice treated with dexamethasone plus DBZ showed a delay and reduction in the incidence of mucous diarrhea, consistent with decreased GSI-induced gut toxicity ($P < 0.001$) (**Supplementary Fig.10 online**). In these experiment, DBZ treatment was maintained for 17 days, when all animals showed severe signs of disease [abdominal stiffness (8/8 mice) and weight loss (8/8) mice]. Upon discontinuation of the drug treatment, the three most affected animals in the DBZ treatment group continued to show accelerated weight loss and died on week three. In contrast, all other 5 C57/Bl6 animals treated with DBZ showed a gradual recovery (improved weight and resolution of abdominal stiffness) one week after discontinuation of the drug. No adverse effects were noted in animals in the vehicle only and dexamethasone only treatment groups.

Importantly, pharmacokinetic analysis of mice treated with dexamethasone for 5 days showed that glucocorticoid treatment reduced the clearance of DBZ *in vivo* (**Supplementary Fig. 12** online). Further analysis of drug metabolism *in vitro* showed a decrease in DBZ metabolism by liver microsomes induced by dexamethasone (**Supplementary Fig. 12** online). These results strongly suggest that the reversal of GSI-induced gastrointestinal toxicity by dexamethasone is not mediated by changes in drug metabolism, but by a protective effect of glucocorticoids in the intestinal epithelium.

How does dexamethasone protect from GSI-induced goblet cell metaplasia? Cell fate decisions in the gut are regulated by a coordinated network of transcription factors that control the proliferation and differentiation of intestinal progenitor cells. In this context, *Klf4*, a transcription factor tumor suppressor gene controlled by NOTCH-Hes1 signaling, functions as a

negative regulator of cell cycle progression and may be involved in the pathogenesis of GSI-induced intestinal toxicity (**Fig.5**), which is characterized by goblet cell differentiation and cell cycle arrest (**Fig. 4** and **Supplementary Fig. 11** online).

A possible explanation to account for the decrease in DBZ-induced gut toxicity by dexamethasone would be an inhibitory effect of glucocorticoids in the expression of *KLF4*. However, experimental analysis of the effects of glucocorticois in *KLF4* expression do not support a direct role of glucocorticoids in the regulation of *KLF4,* as luciferase reporter assays failed to detect regulation of *KLF4* promoter activity by dexamethasone (**Supplementary Figure 17**). These negative results suggest that an indirect effect accounts for the abrogation of DBZ-induced *KLF4* upregulation induced by dexamethasone. To identify possible mediators of glucocorticoid function in the intestinal epithelium we performed gene expression profiling with oligonucleotide microarrays in the intestines of animals treated with vehicle only (DMSO), dexamethasone (15 mg/kg), DBZ (10 μM/kg) or dexamethasone (15 mg/kg) plus DBZ (10 μM/kg) for 5 days. This analysis identified a marked upregulation in *Ccnd2* expression in the intestine of animals treated with dexamethasone, leading us to test the genetic interaction between the effects of dexamethasone in the homeostasis of intestinal epithelial cells and in GSI-induced gut toxicity using *Ccnd2* knockout mice.

As in the case of wild type animals, histological analysis of *Ccnd2* null animals treated with dexamethasone showed a increase numbers of Paneth cells numbers, however, this was accompanied by a reduction of total cell numbers and decreased Ki67 positive cells per crypt (**Figure 6e,f**), which was in contrast with the increased proliferation observed in the gut of glucocorticoid treated controls(**Figure 6e,f**). These results suggest that forced differentiation of the progenitor cells towards the Paneth cell lineage induced by dexamethasone leads to decreased proliferation in the intestinal crypt in *Ccnd2* deficient mice. Moreover, genetic ablation of *Ccnd2* reversed the protective effects of dexamethasone against DBZ-induced goblet cell

metaplasia (**Figure 6e**), which highlights the functional relevance of *Ccnd2* upregulation as a critical mediator of the effects of dexamethasone treatment in the gut. These results, together with the observation that over-expression of *Ccnd2* in AGS cells results in a marked decrease in *KLF4* transcript levels (**Figure 6c**), support that a dexamethasone-*Ccnd2-Klf4* regulatory axis impairs the transcriptional upregulation of *KLF4* upon inhibition of NOTCH1 signaling in the gut and precludes the overt development of goblet cell metaplasia in animals treated with dexamethasone plus DBZ (**Figure 6g**).

The γ-secretase complex is responsible for the processing of several class I transmembrane proteins in addition to NOTCH receptors, including APP, the precursor of amyloidogenic peptides responsible for the pathogenesis of Alzheimer's disease. As a result, GSIs, which block the accumulation of pathogenic Aβ peptides, constitute some of the most promising drugs for the treatment of Alzheimer's disease. However, the development of GSI-induced gut toxicity in preclinical tests has halted the clinical development of GSIs in the treatment of this neurodegenerative disorder. Similarly, the first clinical trial testing the safety and efficacy of blocking NOTCH signaling with a GSI in T-ALL showed a high prevalence of dose-limiting intestinal toxicity. Here we demonstrate that reversal of glucocorticoid resistance in T-ALL cells upon NOTCH inhibition and protection from GSI-induced gut toxicity in animals treated with a GSI plus dexamethasone. These results warrant testing the interaction between GSIs and glucocorticoids in clinical trials evaluating the safety and efficacy of this drug combination in the treatment of T-ALL and may open new therapeutic approaches for the treatment of Alzheimer's disease.

Supplementary methods

Cell viability assays. Viability and cell growth ratios were determined analyzing cell density by a metabolic colorimetric assay (MTT) using the Cell Proliferation Kit I (Roche) in cell lines treated with different antileukemic drugs. The range of concentrations used in these

experiments was: CompE (10^{-12} to 5×10^{-6} M), dexamethasone (10^{-10} to 10^{-4} M), etoposide (10^{-10} to 10^{-4} M), methotrexate (10^{-10} to 10^{-4} M), L-Asparaginase (10^{-8} to 10^{-2} g l^{-1}) and vincristine (10^{-12} to 10^{-6} M).

For the analysis of primary patient samples, cryopreserved T-ALL lymphoblasts were thawed and immediately plated in 1 ml of RPMI1640 media supplemented with 20% FBS and 10 ng ml^{-1} IL7. After 24 hours dead cells were removed using magnetic columns with the Dead Cell Removal Kit (Miltenyi Biotec). Viable cells were counted and plated (2×10^4 cells) in 100 μl of media in the presence if vehicle (DMSO), dexamethasone (100 nM), CompE (100 nM) or dexamethasone (100 nM) plus CompE (100 nM). Viability and cell numbers were analyzed after 48 hours by a WST-1 metabolic colorimetric assay (Roche).

cDNA and shRNA constructs. MigR1 and MigR1-*ICN1* retroviral constructs expressing *EGFP*, and *ICN1 IRES GFP* have been described before [30,31]. MigR1-*Ccnd2* expressing *Ccnd2 IRES GFP* was generated cloning the PCR-amplified mouse *Ccnd2* coding sequence in the MigR1 retroviral vector. The pCS2 ICN-HA vector was generated by cloning into the pCS2 vector the sequence encoding the intracellular domains of *NOTCH1* after PCR amplification from a full length cDNA with primers introducing an ATG initiating codon in the 5' and replacing the termination codon by an HA coding sequence in the 3'. We generated a plasmid (pEP7-HA-HES1) expressing *HES1* by PCR amplification and cloning of a *HES1* cDNA in the pEP7-HA and pMSCV IRES vectors, respectively. pCDNA3.1-MYB expression construct was generated by cloning *Not*I-*EcoR*V *cMYB* cDNA from pCM8-cMYB into the pCDNA3.1 vector. We created the retroviral construct pMSCV-HA-NR3C1 by cloning a pCMV-HA-hGR *BamH*I-*Dra*I fragment containing an HA tagged full length *NR3C1* cDNA, into the pMSCV-puro vector. A hairpin oligonucleotide sequences targeting *NR3C1* (target sequence: 5'-AGCAAGCTTTCCTGGAGCAAAT-3') was expressed from the pGIPZ lentiviral vector. Hairpin oligonucleotide sequences targeting *HES1* (target sequence: 5'-GACAGCATCTGAGCACAGA-3'), *BIM* (target sequence: 5'-AAGGTAGACAATTGCAGCCTG-3'), *BMF* (target sequence: 5'-

GCCCAGAGTAAGGAATGTCTT-3') or the luciferase gene (target sequence 5'-CCTAAGGTTAAGTCGCCCTCG-3') were expressed from the pLKO-puro lentiviral vector.

Retroviral and lentiviral transduction. Retroviral particles were produced and used in spin infections as previously described [32]. Lentivirus production and infections were performed as previously described [33]. Lentiviral particles expressing a luciferase and neomycin phosphotransferase fusion transcript were generated with the FUW-Lucneo vector [34].

DNA microarray analysis. We extracted RNA from duplicate cultures of CUTLL1 cells treated for 24 h with vehicle (DMSO), CompE (100 nM), dexamethasone (1 μM) and CompE (100 nM) plus dexamethasone (1 μM) and prepared samples for analysis with Affymetrix Human U133 Plus 2.0 arrays according to the manufacturer's instructions as previously described [35]. We normalized interarray intensity differences with dChip [36] and selected for analysis the 10,896 probes with least variation among experimental replicas. Genes with synergistic upregulation or downregulation upon CompE plus dexamethasone cotreatment were selected as those with increased or decreased levels of gene expression of at least 30% and 100 units over DMSO, CompE and Dexamethasone treatments.

For microarray analysis of gene expression in mouse intestines we extracted RNA from C57/Bl6 animals treated with vehicle (DMSO), dexamethasone (15 mg kg^{-1}), DBZ (10 μmol kg^{-1}) and dexamethasone (15 mg kg^{-1}) plus DBZ (10 μmol kg^{-1}) by intraperitoneal injection for 5 days. Duplicate samples were analyzed with Affymetrix Mouse 430A_2 arrays according to the manufacturer's instructions as previously described [35]. We normalized interarray intensity differences with Dchip [36] and averaged the expression across duplicate samples. To establish the correlation of expression data and dexamethasone treatment we performed Nearest-neighbor analysis using Signal to Noise statistic: (μ class 0 - μ class 1)/ (σ class 0 + σ class 1), with class 0 corresponding to DMSO and DBZ treated samples and class 1 corresponding to dexamethasone and dexamethasone plus DBZ treated samples.

Quantitative real-time PCR. Total RNA from T-ALL cell lines was extracted with the Perfect Pure RNA Kit (5 Prime) following the manufacturer's instructions. Total RNA from mouse tissues was extracted using Trizol reagent (Invitrogen). cDNA was generated with the Super Script First Strand Synthesis System for RT-PCR (Invitrogen) and analyzed by quantitative real-time PCR using SYBR Green PCR Master Mix (Applied Biosystems) and the 7300 Real-Time PCR System (Applied Biosystems). Relative expression levels were normalized with *GAPDH* expression used as a reference control. Primer sequences are available upon request.

Luciferase reporter assays. We performed *NR3C1* reporter assays in 293T cells cultured in DMEM media supplemented with 10% dialyzed fetal bovine serum in the presence or absence of dexamethasone (1 μM). A luciferase reporter construct (pGL3 *NR3C1 A1 FP11-FP12*) containing the *FP11-FP12* regulatory sequence (5'-CGTAAAATGCGCATGTGTTCCAACGGAAGCACTGG-3') responsible for autoregulation of the *NR3C1* promoter A1 [37] was cotransfected with plasmids expressing *NR3C1* (pcDNA3 *NR3C1*), *MYB* (pcDNA3 *MYB*) and *HES1* (pEP7-*HA-HES1*) and the pRL-CMV *Renilla* luciferase expression plasmid used as normalization and transfection control. *NR3C1* reporter activity and *Renilla* luciferase activity were analyzed 24 h after transfection. For *KLF4*-luciferase reporter assays AGS and HCT116 cells were transfected with pGL2 constructs containing human *KLF4* proximal promoter sequences and plasmids driving expression of HA-tagged ICN1 (pCS2-*ICN1-HA*) or HES1 (pEP7-*HA-HES1*) together with the pRL-CMV *Renilla* luciferase expression plasmid. *Klf4* reporter activity and *Renilla* luciferase levels were analyzed 48 h after transfection.

ChIP-on-chip and quantitative ChIP analysis. HES1 (H-140, Santa Cruz Biotechnology) immunoprecipitates and control genomic DNA of HPB-ALL cells were differentially labeled with Cy3 and Cy5 and hybridized to the Agilent Proximal Promoter Arrays following standard procedures as previously described [38]. To analyze the binding ratios for probes located in the *NR3C1 1B* and *NR3C1 1C* promoters we used the Chip Analytics 1.1 software (Agilent Technologies) and the UCSC Genome Browser. For the analysis of ChIP enrichment of *NR3C1*

1A, 1B and *1C* promoter sequences in CUTLL1 cells and of *KLF4* promoter sequences in HT29 cells we performed real-time PCR using *ACTB* genomic sequence levels as loading control in control genomic DNA (used as reference), and in HES1-specific antibody and IgG control chromatin immunoprecipitates.

Western blot analysis. Antibodies against NOTCH1 (NOTCH1-TAD), activated ICN1 (NOTCH1 Val1744, Cell Signaling Technologies), HES1 (H-140, Santa Cruz Biotechnology), glucocorticoid receptor (E-20, Santa Cruz Biotechnology), BIM (Cell Signaling Technologies); BMF (BD Bioscience); HA epitope (Roche); PARP (H-250, Santa Cruz Biotechnology); cleaved PARP (Asp214) (BD Pharmingen); Ccnd2 (M-20, Santa Cruz Biotechnology), α-tubulin (TU-02, Santa Cruz Biotechnology) and α-actin (C-11, Santa Cruz Biotechnology) were used in immunoblot assays using standard procedures.

Immunohistochemistry. We performed anti Ki67 (Dako), anti lysozyme (Dako) and anti KLF4-immunostaining on formalin-fixed paraffin-embedded tissue sections after antigen retrieval by microwave heating in citrate buffer (pH 6.0) for antibody to Ki67, by proteinase K for lysozyme and by Trilogy (Cell Marque) for antibody to KLF4. After epitope recovery slides were incubated with antibody (anti Ki67 1:50, anti lysozyme 1:500 and anti KLF4 1:500 dilution) overnight at room temperature before antigen detection with diaminobenzidine (DAB) using a Ventana automated staining platform (Ventana).

Pharmacokinetic and drug metabolism studies. To analyze the effects of dexamethasone treatment in DBZ metabolism *in vivo* we injected DBZ (2 μmol kg^{-1}) via tail vein in vehicle-only or dexamethasone (15 mg kg^{-1} for 5 days) pretreated mice and analyzed DBZ concentrations in mouse plasma by LC/MS/MS mass spectrometry in a Sciex API4000 triple quadrupole at serial timepoints. The concentration of DBZ in mouse plasma was determined using a standard curve (analyte peak area *vs.* concentration) generated with calibration standard pools.

To analyze the effects of dexamethasone in the hepatic metabolism of DBZ, we incubated mouse liver microsomes (Xenotech) with DBZ or dexamethasone plus DBZ at 37° C and analyzed DBZ concentrations by LC/MS/MS mass spectrometry in samples taken at serial timepoints using a standard curve prepared in incubation buffer with heat inactivated liver microsomes.

Supplementary references

1. el-Deiry, W.S. Role of oncogenes in resistance and killing by cancer therapeutic agents. *Curr Opin Oncol* **9**, 79-87 (1997).
2. Weinstein, I.B. & Joe, A.K. Mechanisms of disease: Oncogene addiction--a rationale for molecular targeting in cancer therapy. *Nat Clin Pract Oncol* **3**, 448-457 (2006).
3. Bachmann, P.S., Gorman, R., Mackenzie, K.L., Lutze-Mann, L. & Lock, R.B. Dexamethasone resistance in B-cell precursor childhood acute lymphoblastic leukemia occurs downstream of ligand-induced nuclear translocation of the glucocorticoid receptor. *Blood* **105**, 2519-2526 (2005).
4. Bachmann, P.S.*, et al.* Divergent mechanisms of glucocorticoid resistance in experimental models of pediatric acute lymphoblastic leukemia. *Cancer Res* **67**, 4482-4490 (2007).
5. Schmidt, S.*, et al.* Glucocorticoid resistance in two key models of acute lymphoblastic leukemia occurs at the level of the glucocorticoid receptor. *Faseb J* **20**, 2600-2602 (2006).
6. Schmidt, S.*, et al.* Glucocorticoid-induced apoptosis and glucocorticoid resistance: molecular mechanisms and clinical relevance. *Cell Death Differ* **11 Suppl 1**, S45-55 (2004).
7. Schmidt, S.*, et al.* Identification of glucocorticoid-response genes in children with acute lymphoblastic leukemia. *Blood* **107**, 2061-2069 (2006).
8. Schmidt, T.J. & Meyer, A.S. Autoregulation of corticosteroid receptors. How, when, where, and why? *Receptor* **4**, 229-257 (1994).
9. Geley, S., Fiegl, M., Hartmann, B.L. & Kofler, R. Genes mediating glucocorticoid effects and mechanisms of their regulation. *Rev Physiol Biochem Pharmacol* **128**, 1-97 (1996).
10. Geley, S.*, et al.* Resistance to glucocorticoid-induced apoptosis in human T-cell acute lymphoblastic leukemia CEM-C1 cells is due to insufficient glucocorticoid receptor expression. *Cancer Res* **56**, 5033-5038 (1996).
11. Hartmann, B.L.*, et al.* Bcl-2 interferes with the execution phase, but not upstream events, in glucocorticoid-induced leukemia apoptosis. *Oncogene* **18**, 713-719 (1999).
12. Kofler, R. The molecular basis of glucocorticoid-induced apoptosis of lymphoblastic leukemia cells. *Histochem Cell Biol* **114**, 1-7 (2000).

13. Kofler, R., Schmidt, S., Kofler, A. & Ausserlechner, M.J. Resistance to glucocorticoid-induced apoptosis in lymphoblastic leukemia. *J Endocrinol* **178**, 19-27 (2003).

14. Loffler, M.*, et al.* c-Myc does not prevent glucocorticoid-induced apoptosis of human leukemic lymphoblasts. *Oncogene* **18**, 4626-4631 (1999).

15. Obexer, P., Certa, U., Kofler, R. & Helmberg, A. Expression profiling of glucocorticoid-treated T-ALL cell lines: rapid repression of multiple genes involved in RNA-, protein- and nucleotide synthesis. *Oncogene* **20**, 4324-4336 (2001).

16. Ploner, C.*, et al.* Glucocorticoid-induced apoptosis and glucocorticoid resistance in acute lymphoblastic leukemia. *J Steroid Biochem Mol Biol* **93**, 153-160 (2005).

17. Renner, K., Ausserlechner, M.J. & Kofler, R. A conceptual view on glucocorticoid-lnduced apoptosis, cell cycle arrest and glucocorticoid resistance in lymphoblastic leukemia. *Curr Mol Med* **3**, 707-717 (2003).

18. Riml, S., Schmidt, S., Ausserlechner, M.J., Geley, S. & Kofler, R. Glucocorticoid receptor heterozygosity combined with lack of receptor auto-induction causes glucocorticoid resistance in Jurkat acute lymphoblastic leukemia cells. *Cell Death Differ* **11 Suppl 1**, S65-72 (2004).

19. Tonko, M., Ausserlechner, M.J., Bernhard, D., Helmberg, A. & Kofler, R. Gene expression profiles of proliferating vs. G1/G0 arrested human leukemia cells suggest a mechanism for glucocorticoid-induced apoptosis. *FASEB J* **15**, 693-699 (2001).

20. Wei, G.*, et al.* Gene expression-based chemical genomics identifies rapamycin as a modulator of MCL1 and glucocorticoid resistance. *Cancer Cell* **10**, 331-342 (2006).

21. Erlacher, M.*, et al.* BH3-only proteins Puma and Bim are rate-limiting for gamma-radiation- and glucocorticoid-induced apoptosis of lymphoid cells in vivo. *Blood* **106**, 4131-4138 (2005).

22. Abrams, M.T., Robertson, N.M., Yoon, K. & Wickstrom, E. Inhibition of glucocorticoid-induced apoptosis by targeting the major splice variants of BIM mRNA with small interfering RNA and short hairpin RNA. *J Biol Chem* **279**, 55809-55817 (2004).

23. Wang, Z., Malone, M.H., He, H., McColl, K.S. & Distelhorst, C.W. Microarray analysis uncovers the induction of the proapoptotic BH3-only protein Bim in multiple models of glucocorticoid-induced apoptosis. *J Biol Chem* **278**, 23861-23867 (2003).

24. Jang, J.*, et al.* Notch1 confers thymocytes a resistance to GC-induced apoptosis through Deltex1 by blocking the recruitment of p300 to the SRG3 promoter. *Cell Death Differ* **13**, 1495-1505 (2006).

25. Choi, Y.I.*, et al.* Notch1 confers a resistance to glucocorticoid-induced apoptosis on developing thymocytes by down-regulating SRG3 expression. *Proc Natl Acad Sci U S A* **98**, 10267-10272 (2001).

26. Jeon, S.H.*, et al.* A new mouse gene, SRG3, related to the SWI3 of Saccharomyces cerevisiae, is required for apoptosis induced by glucocorticoids in a thymoma cell line. *J Exp Med* **185**, 1827-1836 (1997).

27. Deftos, M.L., He, Y.W., Ojala, E.W. & Bevan, M.J. Correlating notch signaling with thymocyte maturation. *Immunity* **9**, 777-786 (1998).

28. Saito, T.*, et al.* Notch2 is preferentially expressed in mature B cells and indispensable for marginal zone B lineage development. *Immunity* **18**, 675-685 (2003).

29. Tanigaki, K.*, et al.* Notch-RBP-J signaling is involved in cell fate determination of marginal zone B cells. *Nat Immunol* **3**, 443-450 (2002).

30. Weng, A.P.*, et al.* Activating mutations of NOTCH1 in human T cell acute lymphoblastic leukemia. *Science* **306**, 269-271 (2004).

31. Allman, D.*, et al.* Separation of Notch1 promoted lineage commitment and expansion/transformation in developing T cells. *J Exp Med* **194**, 99-106 (2001).

32. Pear, W.S.*, et al.* Exclusive development of T cell neoplasms in mice transplanted with bone marrow expressing activated Notch alleles. *J Exp Med* **183**, 2283-2291 (1996).

33. Moffat, J.*, et al.* A lentiviral RNAi library for human and mouse genes applied to an arrayed viral high-content screen. *Cell* **124**, 1283-1298 (2006).

34. Armstrong, S.A.*, et al.* Inhibition of FLT3 in MLL. Validation of a therapeutic target identified by gene expression based classification. *Cancer Cell* **3**, 173-183 (2003).

35. Basso, K.*, et al.* Reverse engineering of regulatory networks in human B cells. *Nat Genet* **37**, 382-390 (2005).

36. Li, C. & Wong, W.H. Model-based analysis of oligonucleotide arrays: expression index computation and outlier detection. *Proc Natl Acad Sci U S A* **98**, 31-36 (2001).

37. Geng, C.D. & Vedeckis, W.V. c-Myb and members of the c-Ets family of transcription factors act as molecular switches to mediate opposite steroid regulation of the human glucocorticoid receptor 1A promoter. *J Biol Chem* **280**, 43264-43271 (2005).

38. Palomero, T.*, et al.* Mutational loss of PTEN induces resistance to NOTCH1 inhibition in T-cell leukemia. *Nat Med* **13**, 1203-1210 (2007).

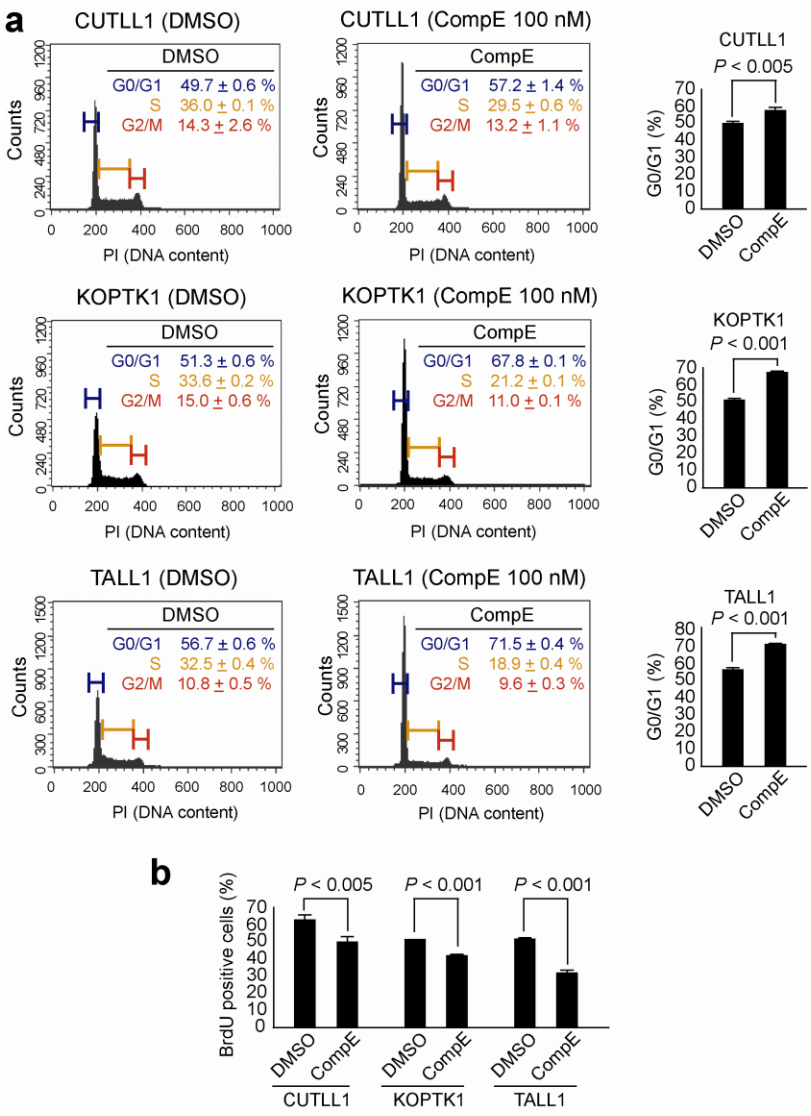

Supplementary Fig. 1. Inhibition of NOTCH signaling induces G1 cell cycle arrest in CUTLL1, KOPTK1 and TALL1 cells. (**a**) DNA content analysis by PI staining of T-ALL cell lines treated with vehicle only (DMSO) or a GSI (CompE 100 nM) for 72 hours shows increased percentage of cells in G0/G1 upon inhibition of NOTCH signaling. (**b**) BrdU incorporation analysis of T-ALL cell lines treated with vehicle only (DMSO) and CompE (100 nM) shows decreased proliferation upon GSI treatment.

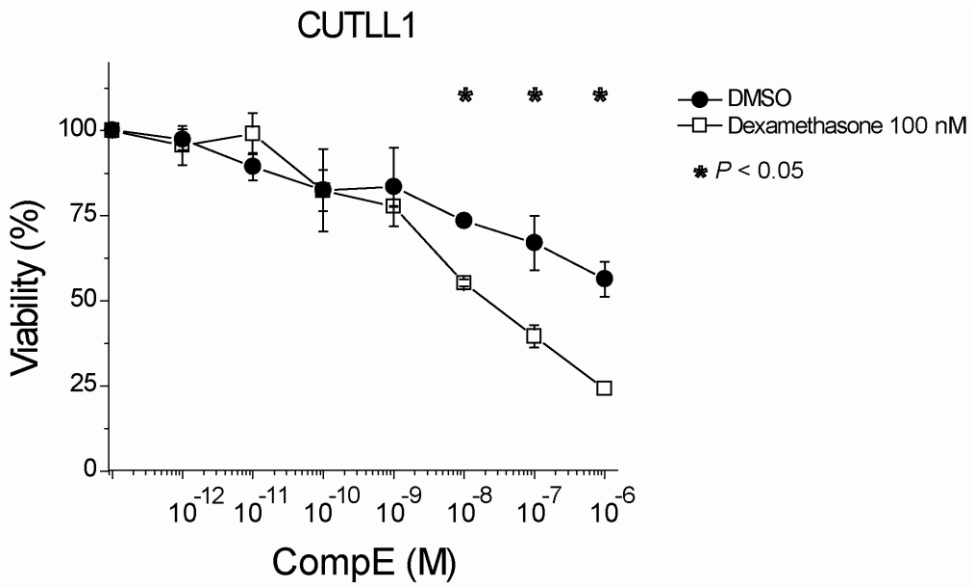

Supplementary Fig. 2. Dose response analysis of CompE in presence of dexamethasone. CUTLL1 cells were treated with increasing doses of CompE in the presence of dexamethasone 100 nM or vehicle only (DMSO) for 72 h. Cell viability was analyzed using an MTT assay.

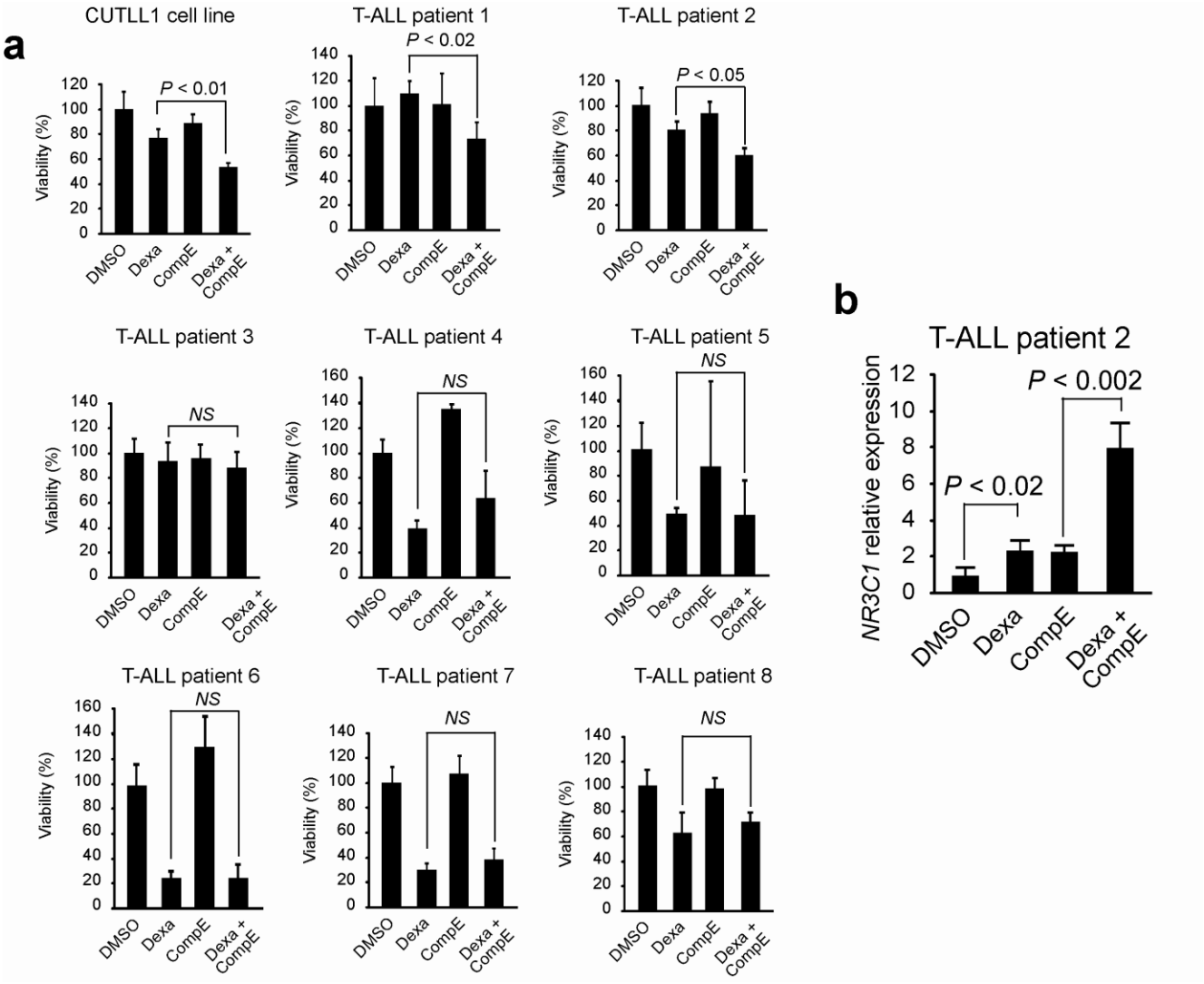

Supplementary Fig. 3. Drug response of relapsed T-ALL primary samples to glucocorticoids and CompE. (**a**) Primary T-ALL lymphoblasts were cultured in presence of DMSO (vehicle control), dexamethasone (1 μM), CompE (100 nM) or dexamethasone (1 μM) plus CompE (100 nM) for 48h. Cell viability was analyzed using an WST-1 assay. Analysis of the CUTLL1 cell line assayed in the same conditions is shown as reference. (**b**) Quantitative RT-PCR analysis of *NR3C1* expression in primary T-ALL lymphoblasts (T-ALL patient 2) showing synergistic upregulation of *NR3C1* transcripts in cells treated with dexamethasone plus CompE.

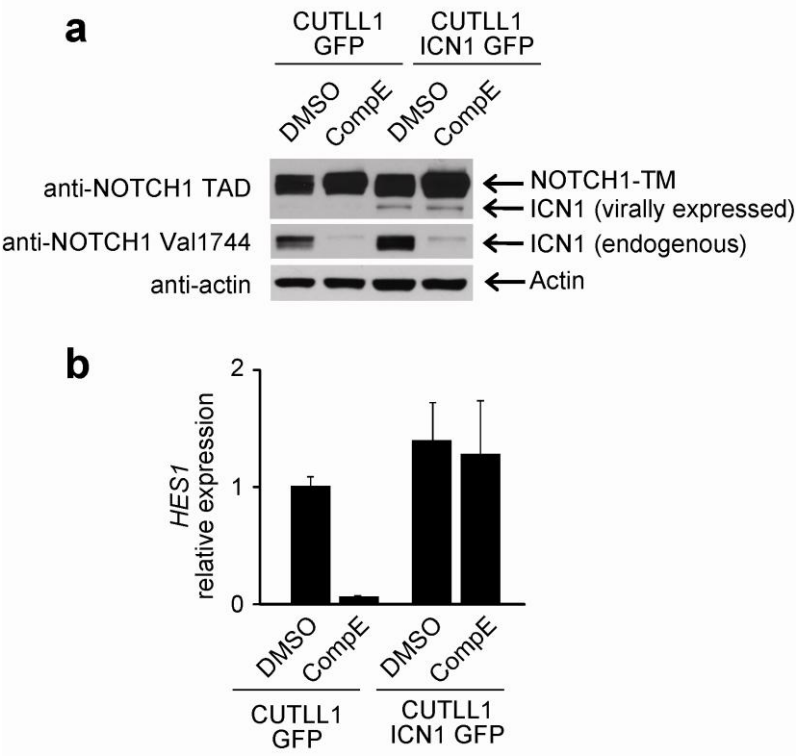

Supplementary Fig. 4. Retroviral expression of ICN1 antagonizes inhibition of NOTCH1 signaling by CompE. (**a**) Western Blot analysis of NOTCH1 (NOTCH1 TAD) in CUTLL1 cells infected with control retroviruses expressing GFP (CUTLL1 GFP) and CUTLL1 cells infected with bicistronic retroviruses expressing ICN1 (CUTLL1 ICN1 GFP). Endogenous ICN1 is masked by the transmembrane form of the receptor (NOTCH1-TM) while the smaller virally expressed ICN1 is detected as a lower molecular weight band. Endogenous ICN1 is visualized using the NOTCH1 Val1744 antibody which recognizes an epitope generated at the site of gamma secretase cleavage but not present in the artificially-generated retrovirally-expressed ICN1 (J. Aster personal communication). Inhibition of γ-secretase cleavage with CompE induces a marked decrease in le levels of endogenous ICN1 (detected with the Val 1744 antibody) but not in retrovirally expressed ICN1 (detected by the TAD antibody). (**b**) RT-PCR analysis of the NOTCH1 target gene *HES1* in CUTLL1 cells infected with retroviruses expressing ICN1 and GFP and control cells expressing GFP only and treated with vehicle only (DMSO) or CompE (100nM) for 24 hours. Inhibition of NOTCH1 signaling with CompE induces marked downregulation of expression of *HES1* in cells infected with control retroviruses expressing GFP. In contrast, cells infected with retroviruses expressing ICN1 and GFP showed sustained *HES1* expression upon inhibition of blocking γ-secretase cleavage with CompE.

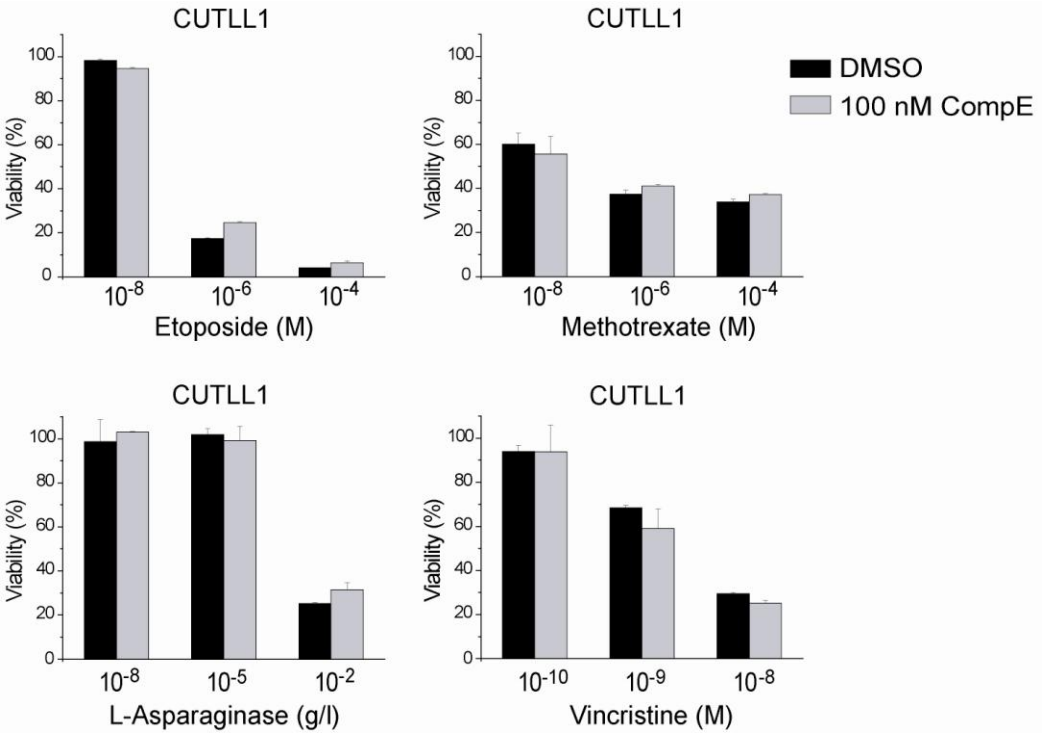

Supplementary Fig. 5. Analysis of the effects of GSI treatment in chemotherapy response. Cell viability analysis in the CUTLL1 cells treated with 100 nM CompE or vehicle only in presence of increasing concentrations of etoposide, methotrexate, L-asparaginase and vincristine. Cell viability was analyzed by an MTT assay and cytotoxicity data was represented as percentage of viable cells compared with non treated controls. Data are means ± SD of triplicate experiments.

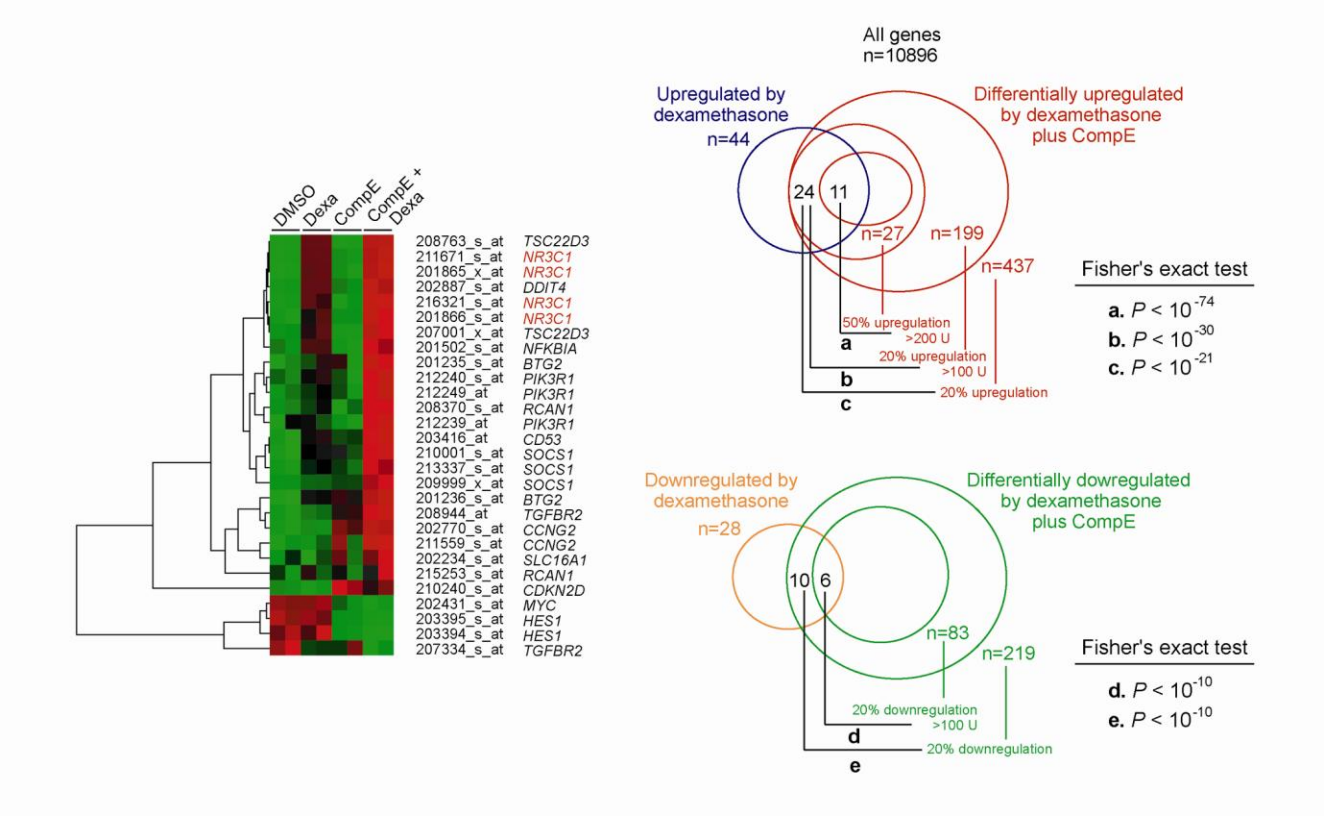

Supplementary Fig. 6. Expression changes induced by dexamethasone plus CompE cotreatment in glucocorticoid regulated genes. The heat map on the left shows relative expression levels in CUTLL1 cells treated with DMSO, dexamethasone, CompE and dexamethasone plus CompE for the most consistent glucocorticoid regulated transcripts identified across multiple microarray studies as described by Schmidt and coworkers [33]. Expression levels are color coded with red indicating higher levels of expression and green indicating lower levels of expression. Genes are displayed as organized by hierarchical clustering using Cluster and Treeview. Venn diagrams on the right show the overlap between genes regulated by dexamethasone treatment and genes differentially upregulated (a, b, c) or downregulated (d, e) by CompE plus dexamethasone cotreatment *vs.* DMSO, CompE or dexamethasone treatment alone. The number of genes in each category and the criteria used for selection of GSI plus glucocorticoid differential regulation *vs*. DMSO, CompE or dexamethasone treatment alone are indicated. The significance of overlap between dexamethasone regulated genes and those showing differential regulation by dexamethasone plus CompE was tested by Fisher's exact test. These results indicate a broad synergistic effect of dexamethasone plus CompE in CUTLL1 cells with increased upregulation or downregulation of glucocorticoid regulated transcripts.

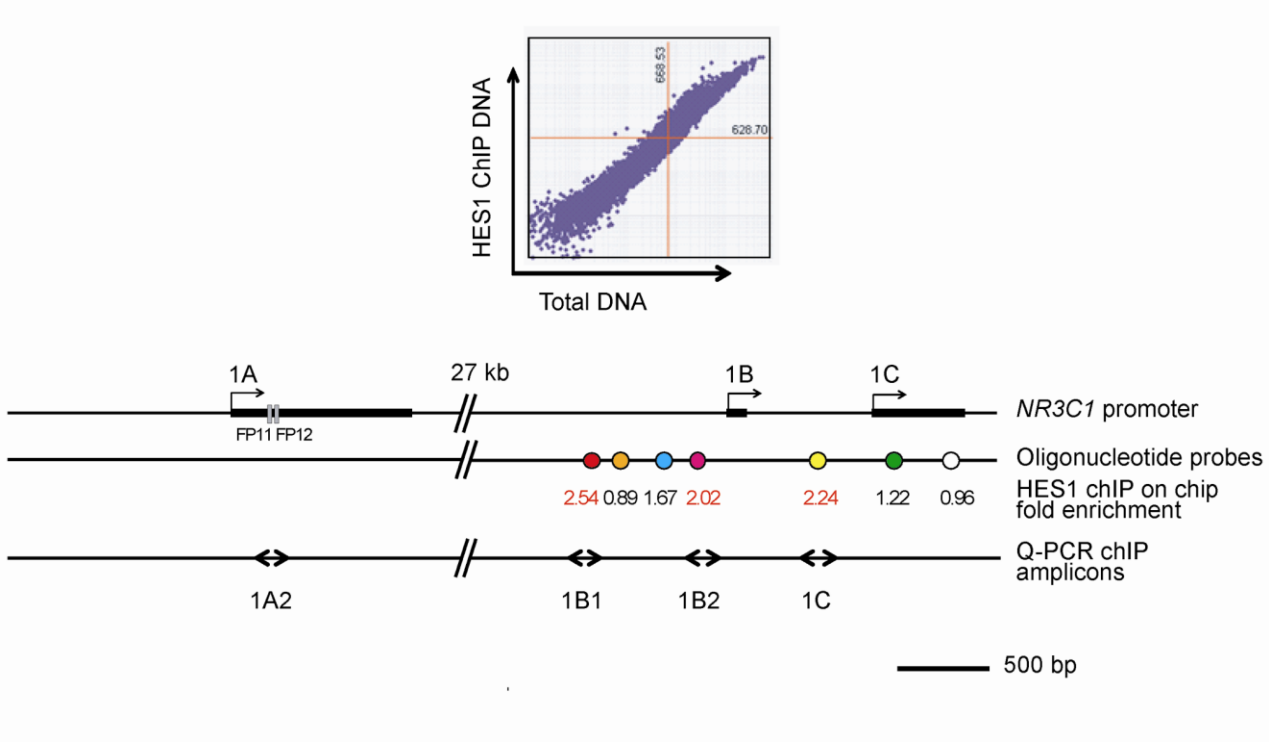

Supplementary Fig. 7. ChIP-on-chip analysis of HES1 binding to the glucocorticoid receptor locus. The scatter plot on the top shows data from HES1 ChIP-on-chip analysis using the Agilent 44K promoter array. The logarithm of fluorescence intensities of HES1 immunoprecipitated chromatin fragments from the HPB-ALL T-ALL cell line in the Y axis plotted against those of total chromatin in the X axis. The diagram at the bottom shows: (i) the structure of the glucocorticoid receptor promoters 1A, 1B and 1C, which are responsible glucocorticoid receptor autoregulation; (ii) the position of each of the seven oligonucleotide probes at the glucocorticoid receptor locus in the Agilent 44K promoter array with their corresponding ChIP-on-chip enrichment values calculated with Agilent Gene Analytics software; and (iii) the position of PCR amplicons used to analyze the enrichment of glucocorticoid receptor promoters 1A, 1B and 1C in HES1 chromatin immunoprecipitates by quantitative PCR in the CUTLL1 T-ALL cell line. FP11 (fingerprint 11) and FP12 (fingerprint 12) are regulatory sequences critically involved in glucocorticoid receptor promoter 1A autoregulation.

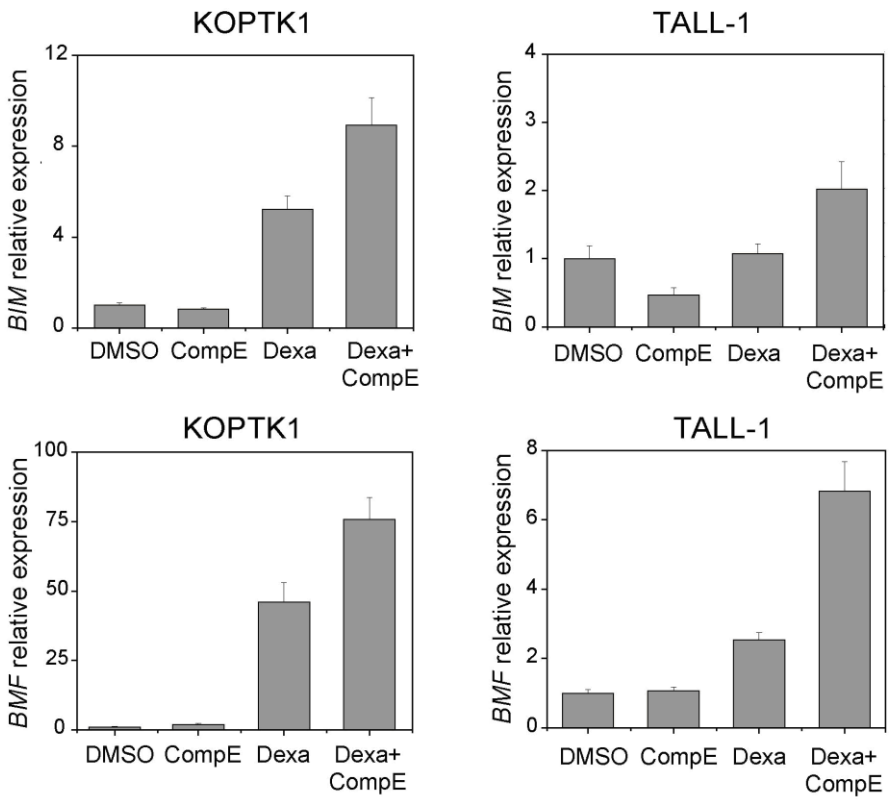

Supplementary Fig. 8. Gene expression analysis of *BIM* and *BMF* in glucocorticoid-resistant T-ALL cells. Quantitative RT-PCR analysis of *BIM* and *BMF* in additional glucocorticoid-resistant T-ALL cells (KOPTK1 and TALL1) showing reversal of glucocorticoid resistance upon treatment with CompE plus dexamethasone. Relative expression levels are shown normalized to those of vehicle only treatment controls. Data are means ± SD of triplicate experiments.

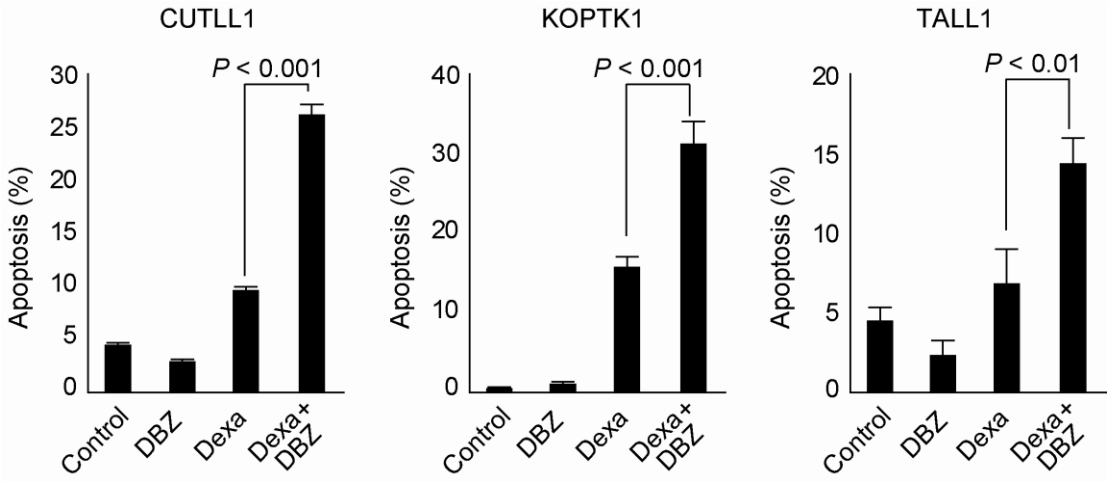

Supplementary Fig. 9. Inhibition of NOTCH1 signaling with DBZ *in vitro* reverses glucocorticoid resistance in T-ALL cells. CUTLL1, KOPTK1 and TALL1 cells were treated with vehicle only (DMSO), dexamethasone 1 μM (Dexa), DBZ 100 nM (DBZ) and dexamethasone 1 μM plus DBZ 100 nM (Dexa + DBZ). Flow cytometry analysis of apoptosis after annexin V/PI staining demonstrates effective reversal of glucocorticoid resistance upon treatment with dexamethasone plus DBZ at 48 hours (KOPTK1) and 72 hours (CUTLL1 and TALL1).

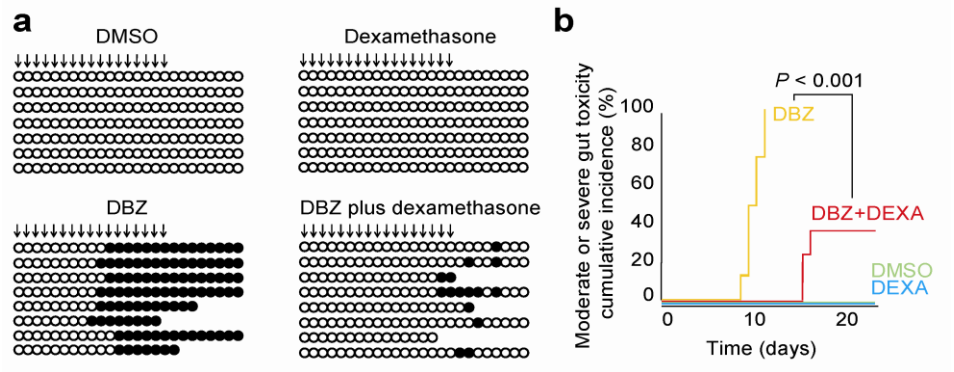

Supplementary Fig. 10. Toxicity analysis of DBZ and dexamethasone in non-leukemia bearing mice. (**a**) C57/Bl6 female mice were treated for 17 days (arrows) with vehicle only (DMSO), dexamethasone (15 mg kg^{-1}), DBZ (10 μM kg^{-1}) or dexamethasone (15 mg kg^{-1}) plus DBZ (10 μM kg^{-1}) via intraperitoneal injection daily. Daily follow up is indicated by circles with clear circles representing asymptomatic mice and solid circles indicating mucous diarrhea. (**b**) Moderate and severe gut toxicity events (moderate toxicity: >3 days of persistent diarrhea; severe toxicity: death) were significantly delayed and decreased in the dexamethasone plus DBZ (DBZ+DEXA) treatment group compared with animals treated with DBZ alone (DBZ).

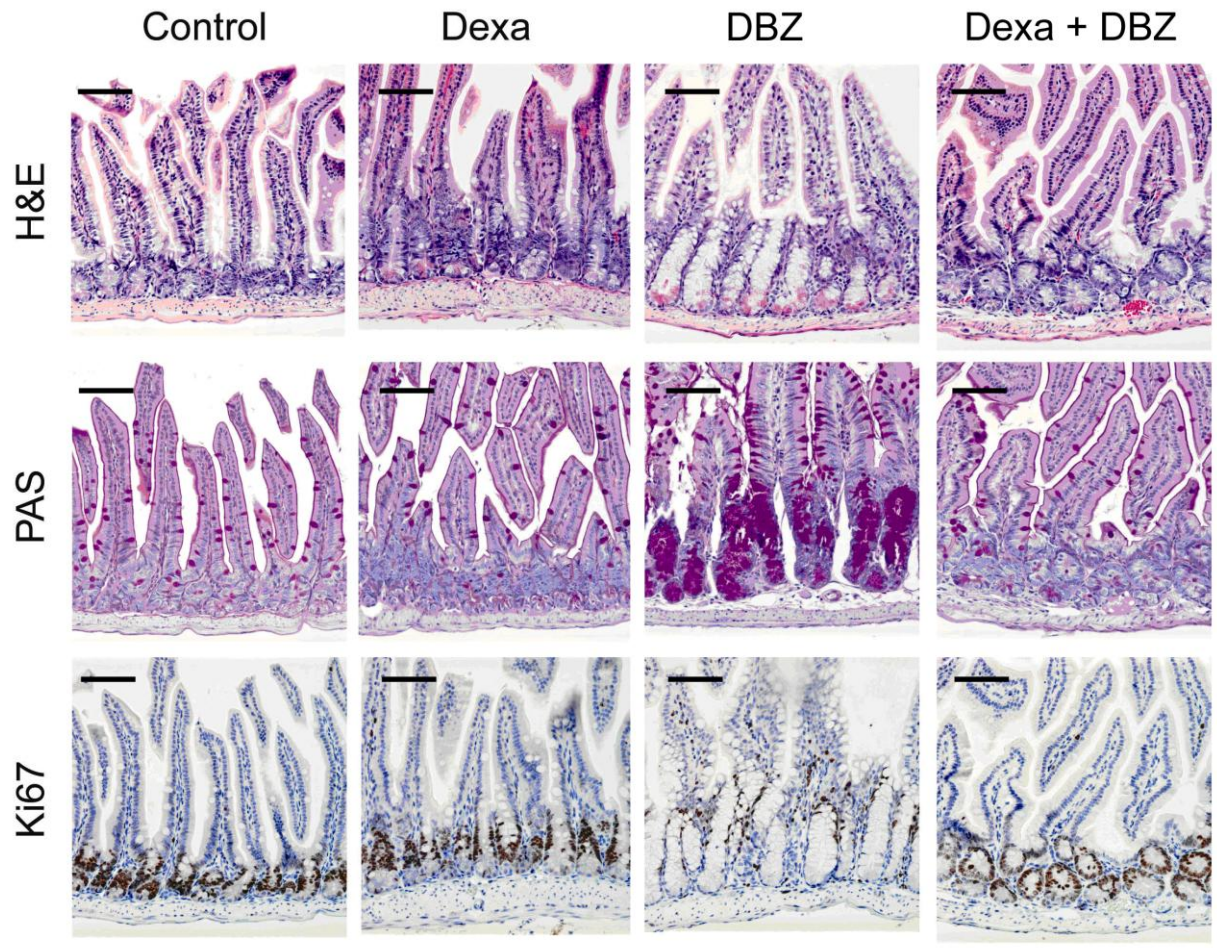

Supplementary Fig. 11. Histopathology of the gut after 10 days of dexamethasone and/or GSI treatment with DBZ. Histological analysis of the small intestine of mice treated for 10 days with dexamethasone (Dexa), a GSI (DBZ), dexamethasone plus GSI (Dexa+DBZ) or vehicle only (control). Hematoxilin eosine (H&E) staining shows marked disorganization of the architecture of the gut in animals treated with DBZ with secretory metaplasia characterized by increased number of goblet cells (PAS staining) and a decrease in the proliferating (Ki67 positive) cells in the crypt. Scale bars represent 100 µm.

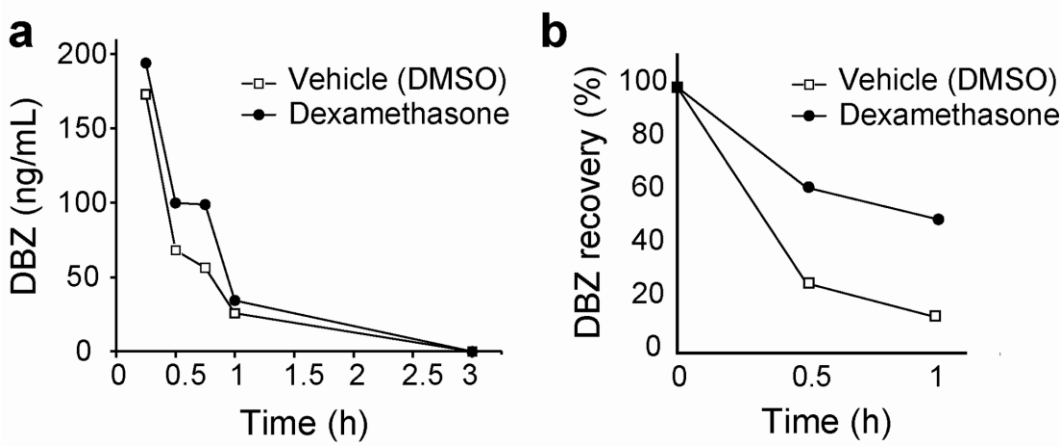

Supplementary Fig. 12. Effects of dexamethasone in DBZ metabolism *in vivo* and *in vitro*. (**a**) Pharmacokinetic analysis of DBZ in animals treated with dexamethasone or vehicle only (DMSO) for 5 days. (**b**) Analysis of DBZ metabolism by liver microsomes *in vitro* showing decreased the metabolization of DBZ in the presence of dexamethasone compared to vehicle controls (DMSO).

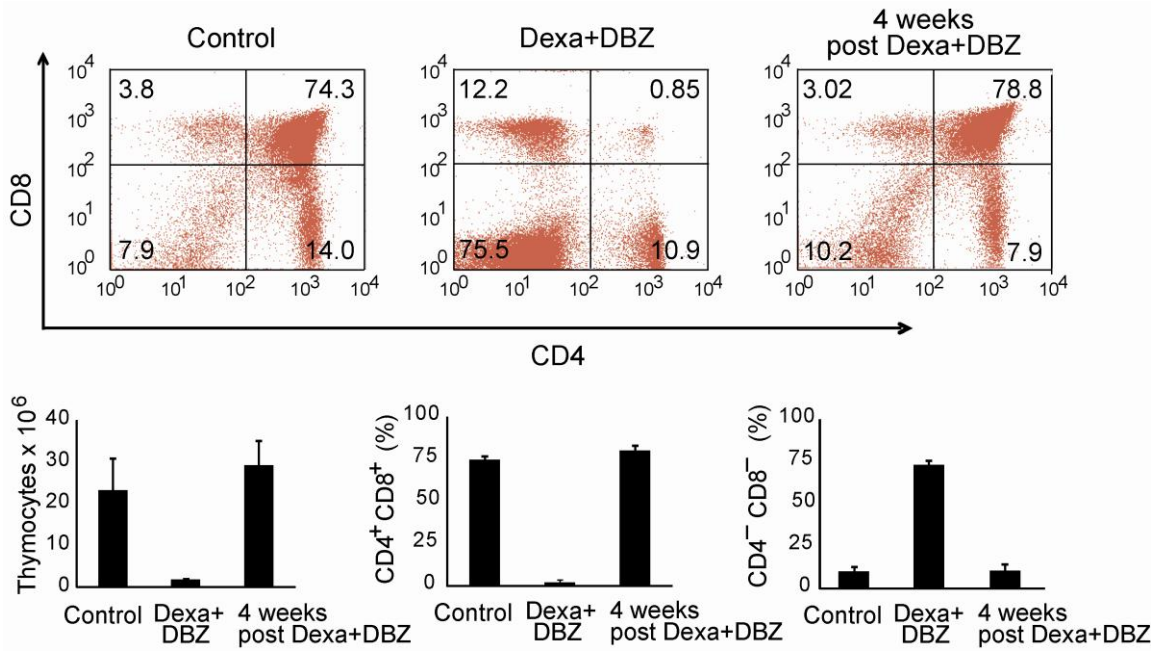

Supplementary Fig. 13. Reversibility of the effects of dexamethasone plus DBZ in the thymus. Flow cytometry analysis of thymocyte populations in animals treated with DMSO (Control) and dexamethasone plus DBZ immediately after 5 days of treatment (Dexa+DBZ); or after 4 weeks off therapy following 5 days of treatment with dexamethasone plus DBZ (4 weeks post Dexa+DBZ). Treatment with dexamethasone plus DBZ for 5 days induced a marked reduction in the cellularity of the thymus and a marked depletion of double positive thymocytes. However, these effects were transient as demonstrated by reconstitution of total thymocyte cell numbers and double positive cells in animals analyzed 4 weeks after the last dose of dexamethasone plus DBZ treatment. Bar diagrams show means ± SD of triplicate experiments.

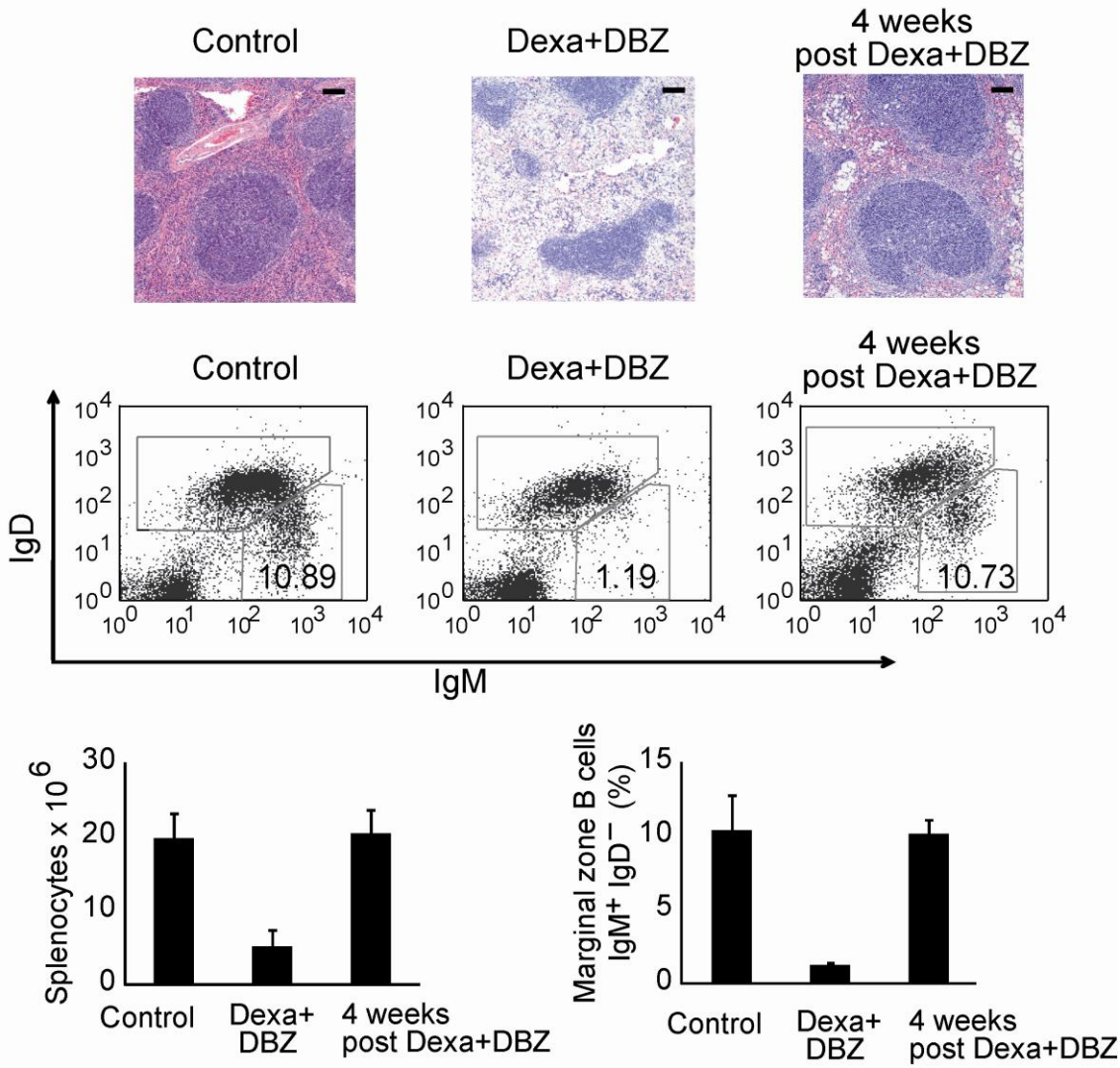

Supplementary Fig. 14. Reversibility of the effects of dexamethasone plus DBZ in the spleen. Histological and flow cytometry analysis of the spleen in animals treated with DMSO (Control) and dexamethasone plus DBZ immediately after 5 days of treatment (Dexa+DBZ); or after 4 weeks off therapy following 5 days of treatment with dexamethasone plus DBZ (4 weeks post Dexa+DBZ). Treatment with dexamethasone plus DBZ for 5 days induced a marked reduction in the cellularity of the spleen with disorganization of the red pulp, atrophy of the lymphoid follicles and ablation of the marginal zone B cells (IgM^+ IgD^- population). Analysis of animals 4 weeks after the last dose of dexamethasone plus DBZ demonstrated that the effects of GSI plus glucocorticoid treatment in the spleen are reversible with restoration of the cellularity and architecture of the organ and repopulation of the marginal zone B-cell compartment. Bar diagrams show means ± SD of triplicate experiments.

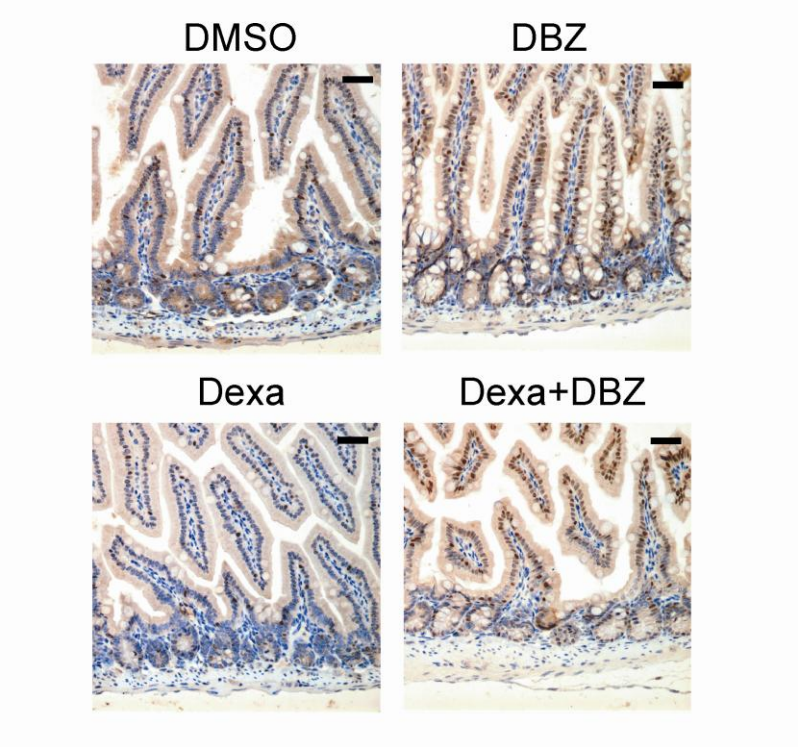

Supplementary Fig. 15. Inhibition of NOTCH signaling *in vivo* with a GSI induces increased expression of the KLF4 goblet cell differentiation factor. Immunoshistochemical analysis of KLF4 expression in the small intestine of mice treated for 5 days with dexamethasone (Dexa), a GSI (DBZ), dexamethasone plus GSI (Dexa+DBZ) or vehicle only (control). Scale bars represent 100 µm.

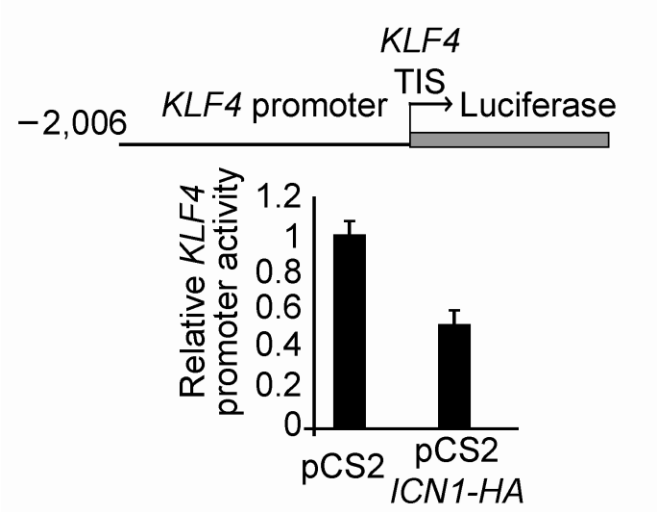

Supplementary Fig. 16. Effects of ICN1 expression in *KLF4* promoter activity in HCT116 colon carcinoma cells. Luciferase reporter assays were performed in HCT116 colon carcinoma cells with a 2,006 base pair *KLF4* reporter construct. Promoter activity is shown relative to an internal control expressing *Renilla* luciferase. TIS: transcription initiation site.

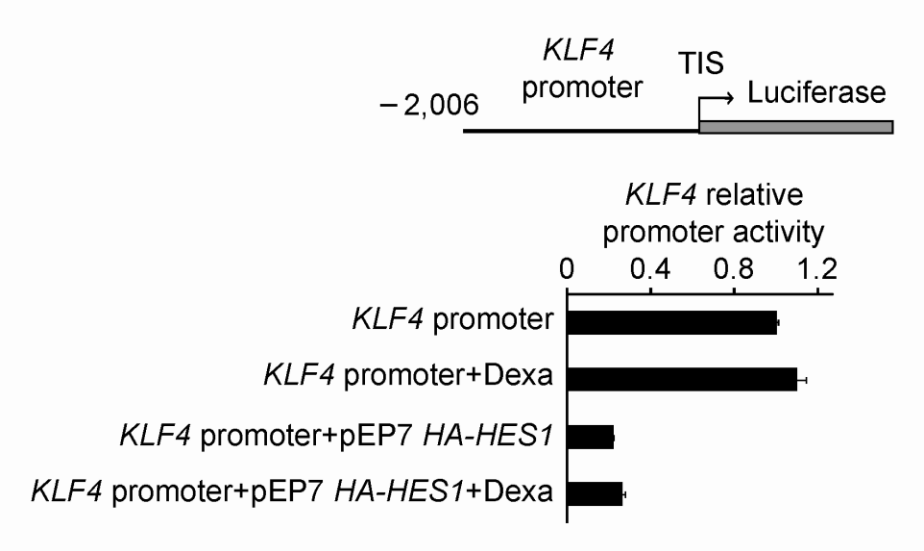

Supplementary Fig. 17. Effects of Dexamethasone and HES1 expression in *KLF4* promoter activity in AGS cells. AGS cells were transfected with a 2,006 base pair *KLF4* reporter construct, a HES1 expression vector (pEP7 *HA-HES1*) or empty vector control and a *Renilla* luciferase expressing construct at 48 hours after treatment with dexamethasone 1 μM or vehicle only for 8 hours. *KLF4* promoter-driven luciferase activity is shown relative to the levels of *Renilla* luciferase used as internal control. TIS: transcription initiation site.